Midgut epithelial responses of different mosquito–*Plasmodium* combinations: The actin cone zipper repair mechanism in *Aedes aegypti*

Lalita Gupta*†, Sanjeev Kumar*†, Yeon Soo Han*‡, Paulo F. P. Pimenta§, and Carolina Barillas-Mury*†¶

*Department of Microbiology, Immunology, and Pathology, Colorado State University, Fort Collins, CO 80523; †Mosquito Immunity and Vector Competence Unit, Laboratory of Malaria and Vector Research, National Institute of Allergy and Infectious Diseases, National Institutes of Health, 12735 Twinbrook Parkway, Rockville, MD 20852; and §Laboratory of Medical Entomology, Centro de Pesquisas René Rachou, Fundação Oswaldo Cruz-Fiocruz Av, Augusto de Lima 1715, Belo Horizonte, MG, CEP 30190-002, Brazil

Edited by Barry J. Beaty, Colorado State University, Fort Collins, CO, and approved January 31, 2005 (received for review December 28, 2004)

In vivo **responses of midgut epithelial cells to ookinete invasion of three different vector–parasite combinations, *Aedes aegypti–Plasmodium gallinaceum*, *Anopheles stephensi–Plasmodium berghei*, and *A. stephensi–P. gallinaceum*, were directly compared by using enzymatic markers and immunofluorescence stainings. Our studies indicate that, in *A. aegypti* and *A. stephensi* ookinetes traverse the midgut via an intracellular route and inflict irreversible damage to the invaded cells. These two mosquito species differ, however, in their mechanisms of epithelial repair. *A. stephensi* detaches damaged cells by an actin-mediated budding-off mechanism when invaded by either *P. berghei* or *P. gallinaceum*. In *A. aegypti*, the midgut epithelium is repaired by a unique actin cone zipper mechanism that involves the formation of a cone-shaped actin aggregate at the base of the cell that closes sequentially, expelling the cellular contents into the midgut lumen as it brings together healthy neighboring cells. Invasion of *A. stephensi* by *P. berghei* induced expression of nitric oxide synthase and peroxidase activities, which mediate tyrosine nitration. These enzymes and nitrotyrosine, however, were not induced in the other two vector–parasite combinations examined. These studies indicate that the epithelial responses of different mosquito–parasite combinations are not universal. The implications of these observations to validate animal experimental systems that reflect the biology of natural vectors of human malarias are discussed.**

Anopheles stephensi | malaria | ookinete | invasion | *Plasmodium berghei*

Anopheline mosquitoes are responsible for transmission of human malarias. The mosquito midgut constitutes a barrier that the parasite must cross to complete its development and infect a new host. Malaria parasites invade the mosquito midgut as a motile form, the ookinete, which develops in the lumen, invades the epithelial cells, and settles beneath the basal lamina. Experimental animal models are instrumental to investigate *Plasmodium*–mosquito interactions and many different vector–parasite combinations have been used (1, 2). The rodent malaria parasite *Plasmodium berghei* can complete its life cycle in anophelines, whereas the chicken malaria parasite *Plasmodium gallinaceum* is compatible with culicines, including *Aedes aegypti* (3). Both model systems are widely used. However, taking into consideration the evolutionary distance between culicines and anophelines and between bird and rodent *Plasmodia*, it is not surprising that these two different experimental systems have given rise to fundamentally different invasion models.

Previous studies of *P. gallinaceum* midgut invasion in *A. aegypti*, using an *in vitro* culture system, reported that ookinetes invade a cell type expressing a high level of vesicular ATPase, different from other epithelial cells, named Ross cells (4). Histochemical and EM analysis indicated that the morphology of these cells differ from other epithelial cells in several ways: They stain poorly with toluidine blue (a basophilic dye), are less osmiophilic in EM sections, contain minimal endoplasmic reticulum, lack secretory granules, and have fewer microvilli (4).

On the other hand, live-imaging studies using interference contrast microscopy in the same *in vitro* culture system revealed that parasites invade midgut epithelial cells with microvilli whose morphology was undistinguishable from that of other cells (5). Epithelial cells suffered drastic changes after invasion; their refractive index decreased, and this was always followed by visible signs of cell deterioration such as nuclear swelling, movement of the nucleus to a more apical position, blebbing of the cell surface, and Brownian motion of cytoplasmic particles. Invaded cells stained positive with eithidium homodimer, indicating rupture of the plasma membrane, and underwent apoptosis, as revealed by activation of a caspase-3-like proteases (5).

Immunofluorescence studies of *A. stephensi* midguts infected *in vivo* by *P. berghei* indicated that ookinetes invade columnar epithelial cell with microvilli, which did not express high level of vesicular ATPase (6). Upon invasion, cells suffered a substantial loss of microvilli and induced nitric oxide synthase (NOS) expression. The damage was extensive and irreversible, as evidence by genomic DNA fragmentation and cell death. An actin string–purse-mediated restitution mechanism allowed the epithelium to "bud off" the damaged cells without losing its integrity (6). In agreement with the observations from Zieler and Dvorak (5), these studies indicated that the morphological changes in invaded cells result from the damage inflicted by the parasite.

It is very difficult to compare the existing information derived from different model systems, because there are many variables such as the use of *in vitro* vs. *in vivo* invasion assays, as well as differences in sample processing and imaging techniques, that could account for some of the contradictory observations. In this paper, we describe the *in vivo* midgut epithelial responses of *A. aegypti* and *A. stephensi* to infection with *P. gallinaceum* and *A. stephensi* with *P. berghei*, based on enzymatic and immunofluorescence stainings of fixed midgut tissues. Fundamental differences in the biochemistry of the cellular responses and the mechanisms of epithelial repair after parasite invasion were found between these animal models of malaria transmission, indicating that the midgut responses to invasion are not universally conserved in different vector–parasite combinations.

Materials and Methods

Mosquitoes and Malaria Infections. *A. stephensi* (NIH strain) and *A. aegypti* (Rex D colony A strain) were reared at 28°C and 80%

This paper was submitted directly (Track II) to the PNAS office.

Abbreviations: DAB, 3,3′-diaminobenzidine; DIC, differential interference contrast; NOS, NO synthase; RT, room temperature.

‡Present address: College of Agriculture and Life Science, Chonnam National University, 300 Yongbong-Dong, Puk-Gu, Gwangju 500-757, Korea.

¶To whom correspondence should be addressed. E-mail: cbarillas@niaid.nih.gov.

www.pnas.org/cgi/doi/10.1073/pnas.0409642102

humidity on a 12-h light–dark cycle. *P. gallinaceum* (8A strain) and *P. berghei* (ANKA 2.34) were maintained by serial passage of infected blood in Leghorn chickens and female BALB/c mice, respectively. Female mosquitoes (4–5 days old) were fed on healthy or malaria-infected chicken or mice.

Midgut Immunostaining. *A. stephensi* midguts were dissected in PBS and fixed in 4% paraformadehyde, as described (6, 7). The same procedure was followed for *A. aegypti*, except that the blocking solution contained 0.2% Triton X-100. Midguts were incubated with primary Abs at 1:300 dilution in PBS plus 0.2% Triton X-100 (PBT) overnight at 4°C and 4 h at room temperature (RT) with Cy5-, Cy3- (Amersham Pharmacia), or Alexa Fluor 488-conjugated secondary Abs (1:500 dilution in PBT), and ToPro3 (Molecular Probes) was used to visualize DNA. Actin was stained by incubating the samples for 20 min at RT with 6.6 μM Alexa Fluor 488-conjugated phalloidin (Molecular Probes). Final images were obtained by using either regular light or fluorescence microscopy and a digital camera or multiple confocal sections. The following Abs were used: mouse antinitrotyrosine mAb (catalog no. 487923, Calbiochem), universal anti-NOS rabbit polyclonal Ab (catalog no. PA1–039, Affinity BioReagents, Neshanic Station, NJ), anti-Pbs21 mAbs (kindly provided by Robert Sinden, Imperial College, London), and anti-Pgs28 mAbs (kindly provided by Louis Miller, National Institutes of Health, Rockville, MD).

***In Vitro* and *in Vivo* Invasion Assay, Midgut Tissue Sections, and Toluidine Staining.** *In vitro* invasion assays were performed as described (4). In brief, blood-fed midguts were dissected 30 h post-blood meal, opened longitudinally, and the blood meal removed. Midgut sheets were suspended in invasion medium. Cultured ookinetes were added to the midguts and centrifuged 1 min at 300 $\times$ *g*, and the pellet was incubated at 26°C for $\approx$30 min, after which the epithelium was washed, fixed, and embedded. *In vivo*-invaded midguts were dissected and immediately fixed in 2.5% glutaraldehyde in 0.1 M sodium cacodylate buffer (pH 7.2) for 24 h, dehydrated with acetone, and embedded. Thick sections (1–2 μm) were attached to glass slides over a hot plate (40°C) and stained with 1% toluidine blue.

3,3′-Diaminobenzidine (DAB) Activity of the Midgut Tissue. Midguts were dissected 24 h post-blood meal, and anti-Pbs21 or anti-Pgs28 Abs were used to detect *P. berghei* and *P. gallinaceum* ookinetes, respectively, as described above. Immunostained midguts were subjected to DAB staining by incubating them at RT with fresh 2.5 mM DAB (Sigma) and 1 mM H_2O_2 (Sigma) in PBS (7). For all experiments *P. berghei*-infected *A. stephensi* midguts served as positive controls. To ensure that the staining was specific for peroxidase activity, midguts were preincubated for 10 min in PBS containing 10 mg/ml 3-amino-1,2,4-triazole (a catalase inhibitor) in PBS (pH 6.5).

Midgut Diaphorase Staining. Midgut NOS activity was determined *in situ* 24 h post-blood meal by using the diaphorase staining. Midguts were dissected, fixed in 4% paraformaldehyde for 1 min at RT, placed on ice-cold PBS, opened longitudinally in PBS to remove the blood meal, and fixed for an additional 30 min at RT in 4% formaldehyde in PBS (formaldehyde fixation is essential for the specific detection of NOS activity by using this reaction) (8, 9). Ookinetes were immunostained, following the procedure described above, transferred to PBS containing 0.2 mM β-NADPH, 0.2% Triton X-100, and 0.2 mM nitroblue tetrazolium, and incubated for 1 h or until a blue–purple color was observed.

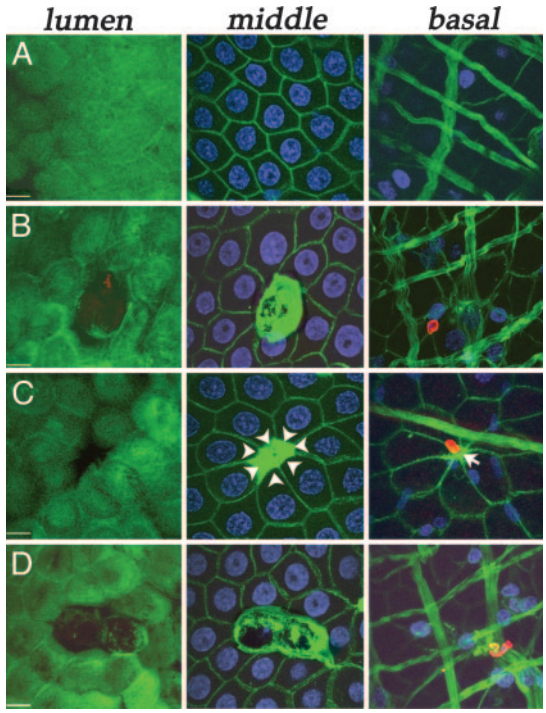

Fig. 1. Immunofluorescence stainings of *P. gallinaceum*-infected *A. aegypti* midguts for actin (green), Pgs28 (red), and nuclei (blue) 24 h after feeding. The midgut epithelium is shown in three different planes: lumen, middle, and basal. (Bars, 5 μm). (*A*) Healthy cells from a bloodfed uninfected midgut. (*B* and *C*) Cells invaded by a single parasite. Notice the accumulation of actin in the middle plane. (*C*) Arrowheads indicate the direction in which the neighboring cells have stretched, and the arrow in the basal plane points to where contact between cells has been reestablished. (*D*) Two adjacent cells invaded by the same parasite.

Results

Actin Organization in Healthy and Parasite-Invaded Cells. *A. aegypti* midguts were analyzed 24 h after feeding on uninfected or *P. gallinaceum*-infected chickens. Ookinetes were stained by using an anti-Pgs28 mouse mAb as described (6). Pgs28 is a surface protein expressed at high levels in *P. gallinaceum* zygotes and ookinetes (10). Actin was visualized by using Alexa488-conjugated phalloidin. To investigate the epithelial changes in response to ookinete invasion, multiple confocal sections were obtained and merged in three groups, representing the luminal, middle, and basal planes, or used to generate lateral views of the epithelial cells. Healthy uninfected cells are densely covered with microvilli and have regular geometrical shapes (usually pentagonal or hexagonal) and a spherical nucleus (Figs. 1*A* and 2*A*). In a lateral view, microvilli are visible on the luminal (lu) surface of healthy cells and the nuclei are round and located at the center of the cell (Fig. 2 *B* and *C*).

Parasite invasion results in damage to the cell surface and loss of microvilli (Fig. 1 *B–D Left*). Neighboring cells lose their symmetry, and a dramatic accumulation of actin is observed (Fig. 1 *B–D Center*). In some cases the area devoid of microvilli is smaller (Fig. 1*C Left*), probably representing a later stage in the repair process, because the invaded cell has lost its nuclei, and the neighboring cells have elongated toward the actin aggregate (Fig. 1*C Center*), which appears to pull them together as it contracts, closing the space left behind by the damaged cell (Fig. 1*C*, white arrowheads). At this stage, the surrounding cells have reestablished contact at the level of the basal lamina (Fig. 1*C Right*, arrow). When a parasite invades more then one

CELL BIOLOGY

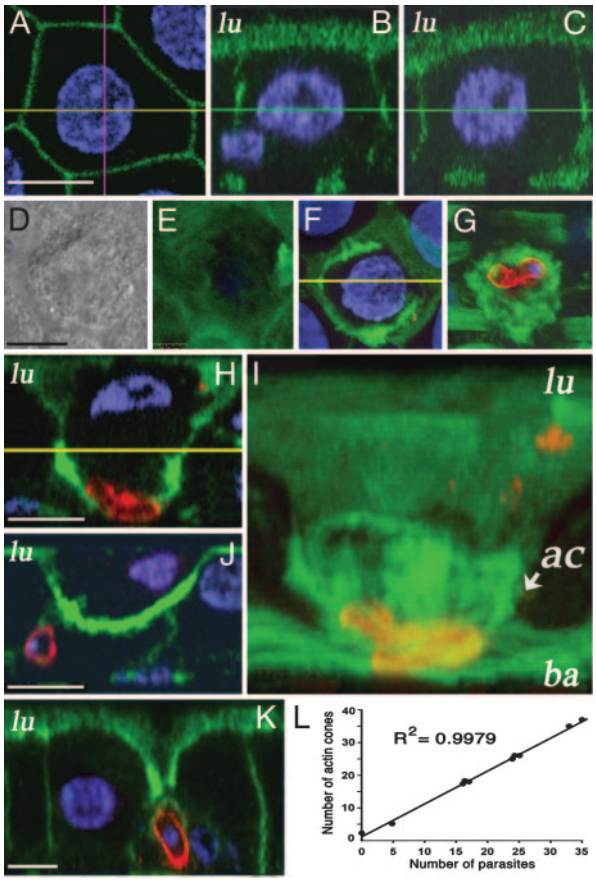

Fig. 2. Detailed analysis of the epithelial repair of *A. aegypti* midgut cells invaded by *P. gallinaceum* 24 h after feeding. (Bar, 5 μm.) Middle plane (*A*) and side (*B* and *C*) views of an uninfected cell from a bloodfed female. The side views were taken across the pink (*B*) and yellow (*C*) lines in *A*. The cell is hexagonal, and the lateral views reveal intact microvilli and a round nucleus (blue) located at the center of the cell. DIC (*D*) and actin staining (*E–G*) (green) of a parasite-invaded cell. Luminal (*E*), middle (*F*), and basal (*G*) planes. (*H*) Side view of the same invaded cell. The lateral membranes are no longer parallel, but converge at the basal plane. Actin accumulates in the basal one-half of the cell, forming a cone structure, and the nucleus is flattened and off-centered. (*I*) 3D reconstruction of the actin cone structure of the same cell. (*J*) Parasite-invaded cell in which the damage has been repaired in from the basal one-half of the epithelium by reestablishing the contact between neighboring cells. (*K*) Parasite-invaded cell at a later stage of repair. Only a small distance is left between healthy cells in the luminal plane; contact has been established in the basal and middle plane. (*L*) Linear correlation (r^2 = 0.9979) between the number of parasites and the number of actin cones in a given midgut (n = 10). lu, luminal surface; ba, basal plane; ac, actin cone.

consecutive cell, each of the damaged cells forms an actin aggregate (Fig. 1*D Center*).

To further investigate the structure of the actin aggregates formed in the invaded cells and their relationship with the surrounding healthy epithelial cells, a series of lateral views were also obtained after 3D reconstruction of confocal stacks. When the actin organization of a parasite-invaded cell (Fig. 2 *D–J*) was carefully analyzed, a lateral view revealed that the sides of the invaded cell were no longer parallel, but had come together at the basal plane (compare Fig. 2*H* with Fig. 2 *B* and *C*). Actin accumulated in the basal one-half of the cell and formed a cone structure, with the cone apex at the base of the cell (Fig. 2 *H* and *I*). The flattened nucleus was off-centered and displaced toward the luminal side (Fig. 2*H*). A 3D reconstruction of the same cell in Fig. 2*I* illustrates the actin cone structure, which extends from the base of the cell (tip of the cone) to the middle of the cell (base of the cone). The cone appears to close sequentially, starting at the tip (Fig. 2*H*, basal plane) and to proceed in a luminal direction, as some intermediate stages were observed, in which intercellular contacts between healthy neighboring cells had been established for the basal one-half of the epithelium, whereas remnants of the invaded cell were still present close to the luminal surface (Fig. 2*J*). At this stage, the surface of the cell was completely devoid of microvilli; the nucleus was irregular and laterally displaced toward the luminal side (Fig. 2*J*). As the healing proceeds, the area of damaged microvilli gets smaller (Figs. 1*C Left* and 2*K*) when the nuclei and cytoplasmic contents of the invaded cell have presumably been expelled into the midgut lumen or undergone autolysis and the contact between healthy neighboring cells has been almost completely reestablished (Fig. 2*K*). Note that at this stage of the healing process, ookinetes come in direct contact with the membranes of the surrounding cells (Fig. 2 *J* and *K*).

The average number of cone structures per midgut increased 8.7-fold in response to *Plasmodium* infection, from 2.8 ± 1.9 (mean ± SD, n = 16) in mosquitoes fed uninfected blood to 24.3 ± 10 (mean ± SD, n = 10) on infected ones. Most cones on infected midguts (228/242 = 94.2%) had an ookinete associated to them. Furthermore, a very strong linear correlation (r^2 = 0.9979) was observed between the number of parasites and the number of actin cones in a given midgut (Fig. 2*L*). All of these findings support the idea that most cone structures are caused by parasite invasion. Other sources of tissue damage during blood feeding could explain the small number of cones not associated with parasites and suggest that this may be a general mechanism of midgut epithelial repair in *A. aegypti*.

***In Vitro* vs. *in Vivo* Ookinete Invasion of Mosquito Midgut Cells.** Tissue sections of *A. aegypti* midguts infected *in vitro* were compared with those of tissues invaded *in vivo* with *P. gallinaceum*, to determine whether these two experimental procedures could result in morphological differences. Toluidine blue-stained sections of *in vitro*-invaded midguts exhibited the same characteristics reported when the Ross cell model was proposed (4); ookinete-invaded cells were less basophilic, had a clear cytoplasm, and contained a large number of vacuoles (Fig. 3*A*). In contrast, cells recently invaded by *Plasmodium in vivo* had a basophilic evenly stained cytoplasm and did not exhibit vacuolation (Fig. 3*B*).

***P. gallinaceum* Invasion of *A. stephensi* Midgut Cells.** *A. stephensi* midgut cells damaged by *P. berghei* invasion protrude and eventually bud off into the midgut lumen as an actin ring constricts at the base of the cell (6). As described above, the actin cone repair process in *A. aegypti--P. gallinaceum* is very different. To establish whether the mechanism of epithelial repair was determined by the parasite or by the mosquito species, a series of experiments were done infecting *A. stephensi* with *P. gallinaceum*. Although this vector/parasite combination does not allow completion of the parasite's life cycle in the mosquito, midgut invasion does take place. Multiple attempts to infect *A. aegypti* midguts with *P. berghei* were unsuccessful (data not shown), confirming previous reports stating that this rodent parasite cannot infect the midgut of this culicine mosquito (1).

A. stephensi midguts were analyzed 24 h after feeding on *P. gallinaceum*-infected chickens. Parasites were stained with anti-Pgs28 Abs (red), and actin (green) was visualized by using Alexa488-conjugated phalloidin. Confocal sections from different planes were merged and lateral views obtained after 3D reconstruction of the stacks. Moderate cell protrusion of invaded cells was observed by differential interference contrast (DIC) (Fig. 3 *C* and *I*, black arrowheads), as well as moderate damage to the microvilli in confocal images from the luminal plane (Fig. 3 *D* and *J*). Actin aggregates were present in the middle and basal

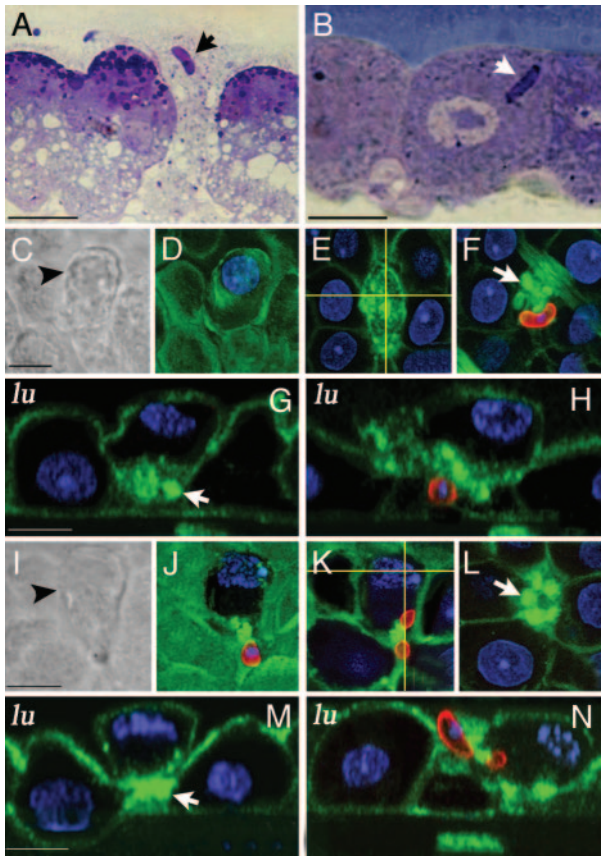

Fig. 3. Epithelial responses to *P. gallinaceum* invasion in *A. aegypti* and *A. stephensi*. Toluidine blue-stained sections of *A. aegypti* midguts infected *in vitro* (*A*) or *in vivo* (*B*) with *P. gallinaceum*. Ookinetes indicated by arrows. (*C–N*) Immunostaining of *P. gallinaceum*-infected *A. stephensi* midguts 24 h after feeding. Tissues were labeled with anti-Pgs28 (red), actin (green), and nuclei (blue). (*C*) DIC of a parasite-invaded cell (arrowhead) that is partially protruding toward the midgut lumen. (*D–H*) Actin staining of the same cell. Loss of microvilli is observed in the luminal plane (*D*), and accumulation of actin is seen in the middle (*E*) and basal (*F*) planes. A basal actin ring (arrow) and protrusion of the invaded cell were confirmed in side views along the horizontal (*G*) and vertical (*H*) lines in *E*. (*I–N*) DIC and immunostainings of an ookinete trapped while invading a midgut cell. Actin accumulated at the point where the parasite is constricted (*K* and *N*). A dramatic loss of microvilli (*J*) and a basal actin ring (*L*) were observed. A basal actin ring (arrow), protrusion of the invaded cell, and detachment from neighboring cells was confirmed in side views along the horizontal (*M*) and vertical (*N*) lines in *K*. (Bars, 5 μm.)

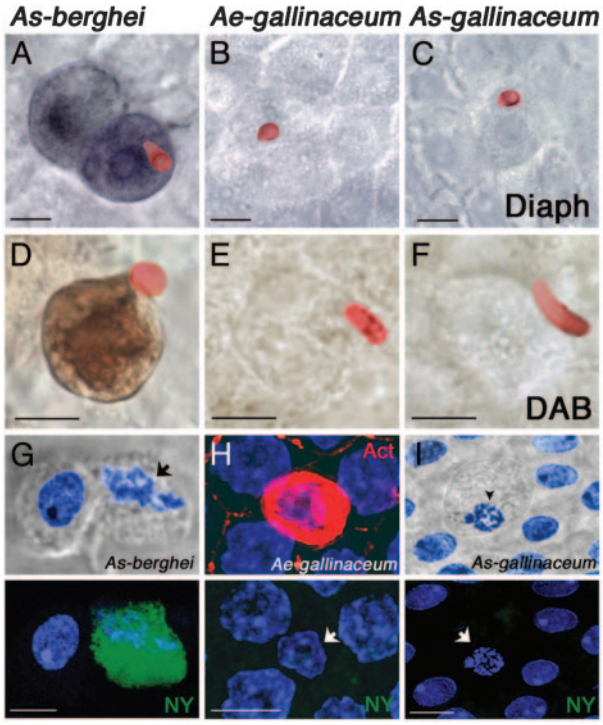

Fig. 4. Biochemistry of midgut epithelial cell responses to parasite invasion 24 h after feeding. (*A–C*) Diaphorase activity assays (purple-blue) and ookinete stainings (red). Diaphorase activity was detected in *A. stephensi* midguts infected with *P. berghei* (*A*), but not in *P. gallinaeum*-infected *A. aegypti* (*B*) or *A. stephensi* (*C*) midguts. (*D–F*) DAB peroxidase activity assays (brown) and ookinete stainings (red). Peroxidase activity was detected in *A. stephensi* midguts infected with *P. berghei* (*D*), but not in *P. gallinaeum*-infected *A. aegypti* (*E*) or *A. stephensi* (*F*) midguts. (*G–I*) Nuclear degeneration (blue, arrow) and cell protrusion by DIC or actin (red) aggregate were used as markers for parasite-induced cell death (*Upper*). Nitrotyrosine staining (green) was detected in *A. stephensi* midguts infected with *P. berghei* (*G Lower*), but not in *P. gallinaeum*-infected *A. aegypti* (*H Lower*) or *A. stephensi* (*I Lower*) midguts. (Bars, 5 μm).

planes (Fig. 3 *E* and *F*). It was clear from the lateral views that actin accumulated in the basal side (Fig. 3*G*, arrow) and that the cell had rounded up as it partially detached from its neighbors. The damaged cell protruded toward the midgut lumen, and, in some areas, the base of the cell was in the same plane as the microvilli of the uninvaded neighboring cells (Fig. 3*H*).

We observed an example where an ookinete was trapped as it crossed the luminal membrane of the cell, so that part of the parasite was intracellular, whereas the rest remained outside the cell (Fig. 3 *I–N*). An actin aggregate was present around the point where the parasite was constricted (Fig. 3 *K* and *N*). Although the invasion process was not completed (Fig. 3*N*), the invaded cell formed a ring at the base (arrows, Fig. 3 *L* and *M*) and detached from its neighbors (Fig. 3*M*). The observed epithelial responses to ookinete invasion are similar to those described for the *A. stephensi–P. berghei* model system, in that invaded cells detach from their neighbors, round up, and form an actin ring that constricts the base. Thus, the general mechanism of epithelial repair appears to be determined by the mosquito vector species and not by the parasite.

Biochemical Responses of Midgut Epithelial Cells to Parasite Invasion. In *A. stephensi*, midgut invasion by *P. berghei* ookinetes induces the expression of NOS, as revealed by increased diaphorase activity (11) and protein expression (6). To establish whether this enzyme was also induced when *P. gallinaceum* invades *A. aegypti* and *A. stephensi* epithelial cells, infected midguts were dissected 24 h after infection, stained with anti-Pgs28 Abs, and assayed for diaphorase activity. As expected, *P. berghei*-invaded *A. stephensi* midgut cells exhibited strong diaphorase staining (Fig. 4*A*). However, *P. gallinaceum*-invaded cells exhibited minimal diaphorase staining, of similar intensity as uninvaded cells, in both *A. aegypti* and *A. stephensi* (Fig. 4 *B* and *C*).

Recent data from our laboratory indicated that tyrosine nitration of parasite-invaded cells in the *A. stephensi–P. berghei* system is a two-step reaction, which requires that NOS induction be followed by increased peroxidase activity (7). Invaded cells undergoing apoptosis, stain strongly when DAB is used as a peroxidase substrate (Fig. 4*D*). None of the *A. aegypti* or *A. stephensi* midgut cells invaded by *P. gallinaceum* had a positive DAB staining, indicating that invasion by this parasite species also does not induce peroxidase activity (Fig. 4 *E* and *F*). *A. stephensi* cells in advanced stages of apoptosis after *P. berghei* infection exhibit nuclear degeneration (Fig. 4*G Upper*, arrow)

CELL BIOLOGY

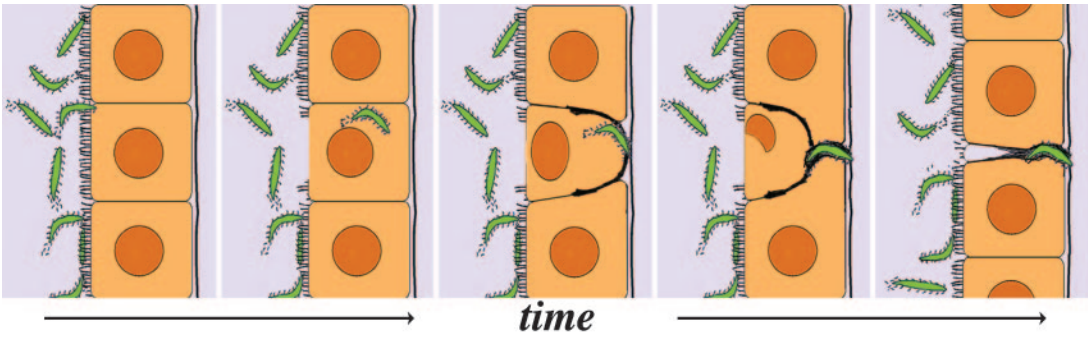

Fig. 5. Diagrammatic representation of the actin cone zipper model of epithelial repair in *P. gallinaceum*-invaded *A. aegypti* midgut. Parasite invasion results in loss of microvilli and actin accumulation in the basal half of the cell. The lateral membranes are no longer parallel, but come together at the basal plane, forming a cone structure. As the nucleus of the invaded cell degenerates, it flattens, is displaced toward the luminal side, and presumably is expelled into the midgut lumen, because it is absent in late stages of repair. Neighboring cells elongate toward the actin cone and come together, closing the space left behind by the damaged cell. The cone closes sequentially, like a zipper, starting at the base and proceeding toward the microvillar surface of the cell.

and stain strongly with anti-nitrotyrosine Abs (Fig. 4*G Lower*). However, tyrosine nitration was never observed in *P. gallinaceum*-invaded *A. aegypti* or *A. stephensi* cells (Fig. 4 *H* and *I Lower*), even when an actin cone (Fig. 4*H Upper*) had formed or when the cell protruded into the lumen and nuclear degeneration was observed (Fig. 4*I Upper*, arrowhead).

Discussion

Epithelial Repair of *A. aegypti* Midguts Cells after *P. gallinaceum* Invasion. The diagram in Fig. 5 illustrates the *in vivo* epithelial responses of *A. aegypti* to *P. gallinaceum* invasion. These experimental observations led us to propose a different mechanism of epithelial repair, the actin cone zipper model. This model proposes that: (*i*) healthy uninfected cells are densely covered with microvilli, have regular geometrical shapes, their lateral membranes are parallel to each other, and their nuclei are spherical and centered. (*ii*) After parasite invasion, cells suffer dramatic changes. The nucleus becomes smaller and flattens into an oval shape or becomes amorphous; it is displaced toward the luminal side of the cell or is completely absent at later stages of repair. Actin accumulates along the basal one-half of the lateral membranes. The sides of the cell are no longer parallel but come together at the base, forming a cone structure. (*iii*) Cells in intermediate stages of repair suggest that this cone closes sequentially, like a zipper, starting at the basal plane and proceeding toward the luminal plane. As the sides of the invaded cell come together, the contents of the damaged cell are presumably expelled into the midgut lumen or undergo autolysis. The healthy neighboring cells gradually come together, closing the space between them, and as they do so, their lateral membranes come in close contact with the invading ookinete. Actin accumulates in the lateral membranes that are actively migrating toward each other, but this aggregate is no longer observed in areas where the contact between healthy cells has been reestablished.

Invasion Route in the *A. aegypti–P. gallinaceum* System. Most authors agree that *P. gallinaceum* ookinetes take an intracellular invasion route when invading *A. aegypti* midgut cells (4, 5, 12), and the present study confirms these observations. In previous EM studies, however, ookinetes were found to migrate both within and between midgut epithelial cells (13). The intracellular parasites were usually near the luminal surface and the intercellular ones near the basal area. Based on this finding, it was suggested that after invasion the parasite moved from the intracellular environment to the intercellular space before reaching the basal lamina (13). The proposed actin cone zipper model is consistent with the experimental observations described but offers an alternative interpretation; the apparent intercellular location would result from the movement of healthy neighboring cells toward each other. In intermediate and late stages of repair, their lateral membranes come in close contact with the parasite when the contents of the damaged cell are expelled into the midgut lumen or lysed.

Different Invasion Models Proposed for the *A. aegypti–P. gallinaceum* System. Previous studies have been controversial regarding the identity of the cells invaded by the parasite and the midgut epithelial responses to invasion. Both the Ross cell model and live imaging studies agree that parasite-invaded cells look different (4, 5), but the key issue is whether the invaded cells represent a special epithelial cell-type preferentially invaded by ookinetes or whether the differences after invasion result from the cellular responses to the damage inflicted by the parasite (14–16).

The comparison of toluidine blue-stained sections from epithelial cells invaded *in vitro* and *in vivo* revealed important differences in cell morphology between these two experimental strategies (Fig. 3 *A* and *B*). In midgut epithelial sheets that underwent parasite invasion *in vitro*, invaded cells were heavily vacuolated and had a clear cytoplasm (Fig. 3*A*) as reported (4). The fact that extensive vacuolation was also observed in uninvaded cells suggests that, under this *in vitro* culture conditions, the midgut epithelial sheets were probably subjected to osmotic stress (Fig. 3*A*). When midgut invasion took place *in vivo*, no vacuoles were present, and recently invaded cells did not exhibit any of the characteristic features of the Ross cells (Fig. 3*B*). Their cytoplasm stained well and was not different from that of healthy neighboring cells. These observations are in agreement with previous EM studies of *in vivo*-infected midguts in which invaded cells were not found to be vacuolated and their cytoplasm was not electron lucent (12, 13).

Taken together, all these previous observations, as well as the actin-mediated epithelial repair just described, favor the interpretation that the morphological differences observed in parasite-invaded cells reflect cell damage caused by invasion. The clear cytoplasm in *in vitro*-invaded cells probably results from loss of cytoplasmic content into the media, because this loss of material has been well documented during live imaging of the invasion process *in vitro* (5). Thus, the Ross cell probably represents a cell that has lost its integrity and some of its cytoplamic contents after parasite invasion.

Universality of Invasion Models in Different Vector–Parasite Species. Previous studies indicate that *P. berghei* invasion of *A. stephensi* (6, 17) and *A. gambiae* (7, 18) midgut epithelial cells is intracel-

lular and results in cell damage. The intracellular passage is evident by the cytoplasmic release Pbs21 (6), a glycosylphosphatidylinositol-anchored ookinete surface protein (19), and from previous EM studies (17). These observations have recently been confirmed by real-time *in vivo* analysis of midgut invasion by using transgenic *P. berghei* ookinetes expressing GFP (20).

There are several similarities between the previously proposed "time bomb model of ookinete invasion," using the *A. stephensi–P. berghei* system (6), and the newly proposed actin cone zipper repair mechanism for the *A. aegypti–P. gallinaceum*: (*i*) Parasites invade intracellularly; (*ii*) they cause damage to the invaded cell; and (*iii*) initially, the epithelium is repaired via an actin-mediated restitution mechanism that involves cellular displacements, but does not involve cell proliferation. There are however important differences: In *A. stephensi*, damaged cells detach from their neighbors and form an actin ring that closes as the cell remnant buds off into the midgut lumen. This budding off mechanism is apparently characteristic of this mosquito species, as the same repair was observed when cells were invaded by either *P. berghei* or *P. gallinaceium* parasites. Recent *in vivo* studies have confirmed that *P. berghei*-invaded *A. stephensi* and *A. gambiae* midgut cells protrude apically, undergo chromatin condensation and apoptosis (20) in agreement with the time bomb model (6). In contrast, *A. aegypti* midgut cells damaged by *P. gallinaceum* remain associated with their neighbors, forming a basal actin cone that extrudes the cellular contents as it brings together healthy neighboring cells.

Given the differences found between experimental systems, the issue of how closely these animal models resemble the responses of natural mosquito vectors to human malaria parasites becomes of central importance. Early EM studies of *Plasmodium falciparum* (NF54 strain) invasion of *A. stephensi* midguts concluded that ookinetes invaded via an intercellular route and did not cause cell damage (17, 21). These conclusions were based on very few invasion events from ookinetes that were located in close proximity to the basal lamina. A recent study examined 5,963 giemsa-stained histological sections obtained from 18 *A. stephensi* midguts infected with *P. falciparum* (3D7A strain) (22). Ookinetes were clearly visible within midgut epithelial cells. No evidence was found for the existence of a distinct cell type with characteristic morphological features that was preferentially invaded by ookinetes, but invasion resulted in dramatic changes such as differential staining, nuclear condensation and fragmentation, vacuolization, loss of microvilli, and extrusion into the midgut lumen, in agreement with the time bomb model (22). This study indicates that *P. berghei* and *P. falciparum* follow the same invasion route and elicits a similar mechanism of epithelial repair in *A. stephensi*.

In vivo analysis of midgut invasion by *P. berghei* ookinetes has also revealed that although invasion is clearly intracellular, in the basal planes, parasites exit the epithelial cells by migrating in a basal direction in between cells, through the intercellular spaces or at three-cell junctions (20). In *P. falciparum* (3D7A strain) infections, intercellular parasites were found in the basal regions, but in 86% of the cases they were associated with epithelial cells exhibiting altered morphology (when multiple serial sections were analyzed), and frequently parasites and extruding cells were not present within the same section (22). Thus the discrepancy with previous EM studies could be due to a sampling problem; however it is also possible that different *P. falciparum* strains (NF54 vs. 3D7A) elicit different responses.

In situ diaphorase staining under conditions that reveal NOS activity and peroxidase-mediated DAB staining used in combination with parasite detection by immunofluorescence were useful markers to compare the biochemistry of the reactions elicited by different vector–parasite combinations. Both activities are highly induced in *A. stephensi* and *A. gambiae* in response to *P. berghei* invasion (7); however they are not present in *P. gallinaceum*-invaded *A. aegypti* midgut cells. Surprisingly, although *A. stephensi* epithelia was also repaired through a budding-off mechanism when invaded by *P. gallinaceum*, there was no evidence for activations of NOS or peroxidase, suggesting that these enzymatic inductions were not triggered merely in response to the physical damage by the parasite, but by specific signaling triggered by *P. berghei* ookinetes. Understanding the molecular basis of this specific signaling pathway deserves further investigation.

We thank Drs. Jose Ribeiro, Jesus Valenzuela, and Jim Dvorak for critically reviewing the manuscript and providing comments and suggestions and Drs. Robert Gwadz, Thomas Wellems, and Thomas Kindt for support and encouragement. The initial part of this work at Colorado State University was funded by a research grant (R01AI45573) from the National Institutes of Health. P.F.P.P. was funded by grants from Conselho Nacional de Desenvolvimento Tecnológico, Fundação de Apoio a Presquisas de Minas Gerais, and Fundação Oswaldo Cruz.

1. Vernick, K. D., Fujioka, H., Seeley, D. C., Tandler, B., Aikawa, M. & Miller, L. H. (1995) *Exp. Parasitol.* **80,** 583–595.
2. Yoeli, M., Vanderberg, J., Upmanis, R. S. & Most, H. (1965) *Nature* **208,** 903.
3. Thathy, V., Severson, D. W. & Christensen, B. M. (1994) *J. Parasitol.* **80,** 705–712.
4. Shahabuddin, M. & Pimenta, P. F. (1998) *Proc. Natl. Acad. Sci. USA* **95,** 3385–3389.
5. Zieler, H. & Dvorak, J. A. (2000) *Proc. Natl. Acad. Sci. USA* **97,** 11516–11521.
6. Han, Y. S., Thompson, J., Kafatos, F. C. & Barillas-Mury, C. (2000) *EMBO J.* **19,** 6030–6040.
7. Kumar, S., Gupta, L., Han, Y. S. & Barillas-Mury, C. (2004) *J. Biol. Chem.* **279,** 53475–53482.
8. Truman, J. W., De Vente, J. & Ball, E. E. (1996) *Development (Cambridge, U.K.)* **122,** 3949–3958.
9. Wildemann, B. & Bicker, G. (1999) *J. Neurobiol.* **39,** 337–346.
10. Duffy, P. E., Pimenta, P. & Kaslow, D. C. (1993) *J. Exp. Med.* **177,** 505–510.
11. Luckhart, S., Vodovotz, Y., Cui, L. & Rosenberg, R. (1998) *Proc. Natl. Acad. Sci. USA* **95,** 5700–5705.
12. Vernick, K. D., Fujioka, H. & Aikawa, M. (1999) *Exp. Parasitol.* **91,** 362–366.
13. Torii, M., Nakamura, K., Sieber, K. P., Miller, L. H. & Aikawa, M. (1992) *J. Protozool.* **39,** 449–454.
14. Cociancich, S. O., Park, S. S., Fidock, D. A. & Shahabuddin, M. (1999) *J. Biol. Chem.* **274,** 12650–12655.
15. Han, Y. S. & Barillas-Mury, C. (2002) *Insect Biochem. Mol. Biol.* **32,** 1311–1316.
16. Shahabuddin, M. (2002) *Trends Parasitol.* **18,** 157–161.
17. Meis, J. F., Pool, G., van Gemert, G. J., Lensen, A. H., Ponnudurai, T. & Meuwissen, J. H. (1989) *Parasitol. Res.* **76,** 13–19.
18. Danielli, A., Kafatos, F. C. & Loukeris, T. G. (2003) *J. Biol. Chem.* **278,** 4184–4193.
19. Blanco, A. R., Paez, A., Gerold, P., Dearsly, A. L., Margos, G., Schwarz, R. T., Barker, G., Rodriguez, M. C. & Sinden, R. E. (1999) *Mol. Biochem. Parasitol.* **98,** 163–173.
20. Vlachou, D., Zimmermann, T., Cantera, R., Janse, C. J., Waters, A. P. & Kafatos, F. C. (2004) *Cell Microbiol.* **6,** 671–685.
21. Meis, J. F. & Ponnudurai, T. (1987) *Parasitol. Res.* **73,** 500–506.
22. Baton, L. A. & Ranford-Cartwright, L. C. (2004) *Parasitology* **129,** 663–676.